PNAS
www.pnas.org

Supplementary Information for

Compulsive Drug Use is Associated with Imbalance of Orbitofrontal- and Prelimbic- Striatal Circuits in Punishment-Resistant Individuals

Yuzheng Hu, Betty Jo Salmeron, Irina N. Krasnova, Hong Gu, Hanbing Lu, Antonello Bonci, Jean L. Cadet, Elliot A. Stein, Yihong Yang

Yihong Yang: yihongyang@intra.nida.nih.gov; Yuzheng Hu: huyuzheng@zju.edu.cn

This PDF file includes:

www.pnas.org/cgi/doi/10.1073/pnas.1819978116

1. Imaging data acquisition and preprocessing

MRI data were acquired on a Bruker Biospin 9.4T scanner (Bruker Medizintechnik, Karlsruhe, Germany) using a surface circular coil and birdcage volume transmit coil. High-resolution anatomical images were acquired using a Rapid Acquisition with Relaxation Enhancement (RARE) sequence (repetition time (TR) = 2200 ms, FOV = 35×35 mm^2, slice thickness = 0.5 mm, slice number = 30). FMRI data were acquired using a T2*-weighted EPI sequence (TE = 13 ms, TR = 1000 ms, FOV = 35 × 35 mm^2, matrix size = 64×64, slice thickness = 1 mm, slice number = 15), initiated 90 minutes post anesthesia induction (1). FSL (https://fsl.fmrib.ox.ac.uk) and AFNI (2) were used in fMRI data preprocessing, which included discarding the first 4 volumes, slice timing correction, motion correction, and spatial smoothing (blurred to a full-width at half-maximum of 0.8 mm). Independent component analysis (ICA) was applied to decompose the data into 30 components. Components with the following characteristics were identified as noise components: 1) signals dominated by a single frequency or by high frequencies above 0.3 Hz; 2) signals with obvious spikes in the time domain; and 3) signals with equal power distribution in the whole frequency range and spatially scattered in the brain. Noise components were regressed out and a bandpass filter (0.01 - 0.25Hz) was applied to the de-noised data before functional connectivity calculation (3). The fMRI images were aligned to their corresponding T2-weighted image and normalized to a 3D template space aligned with a rat stereotaxic atlas (4) using Advanced Normalization Tools (https://stnava.github.io/ANTs/). Seed-based rsFC was calculated by correlating the time course of a seed region with the voxel-wise time course in the rest of the brain. The resultant correlation coefficients (r) were transformed to z-values using Fisher's r-to-z transformation $z = 0.5 * \log \frac{1+r}{1-r}$.

2. Computational modelling of SA data

The ratio of drug intake on the last shock day to that on the last SA training day (day 20) was used to characterize compulsive behavior. As significant day-to-day drug intake variability is seen across animals, to mitigate these fluctuations and determine stable drug intake, infusion data during the SA training and punishment phases were modeled for each rat using formula 1 and 2, respectively. Mode fitting was implemented with the Matlab function "fit" (MATLAB and Statistics Toolbox Release 2017b, The MathWorks, Inc., Natick, MA, USA). SI **Fig. S2** shows exemplar patterns of METH infusions in the SA training and punishment phases together with the computationally fitted data (solid lines).

For infusions during SA: $\mathrm{Y} = \left(\frac{1}{1+e^{-x*a1}} - 0.5 \right) * b1 + c1$ (1),

where Y is the infusion number and x ∈ [0, 19] is the 20 experiment days; a1, b1, and c1 are parameters determined specifically for each rat by mode fitting.

For infusions during SA+FS: $\mathrm{Y} = e^{-x} * b2 + c2$ (2),

where Y is the infusion number of the last SA day with the five punishment days, and x ∈ [0, 5] is the experiment days; b2 and c2 are parameters determined specifically for each rat by mode fitting.

3. Animal preparation for fMRI experiment

For magnetic resonance imaging (MRI) scans, animals were anesthetized with a combination of isoflurane (Piramal Critical Care Inc., Bethlehem, PA, USA) and dexmedetomidine hydrochloride (Zoetis Services LLC, Parsippany, NJ, USA). Briefly, anesthesia was induced with 2% isoflurane and a 0.02 mg/kg subcutaneous bolus injection of dexmedetomidine. Rats were secured in an animal holder with a bite bar and core body temperature was maintained at 37±1^{o}C with a water-circulating heating pump. Heart rate and blood oxygenation levels were continuously monitored using a noninvasive pulse oximetry attached to the animal's hind foot, while respiration rate was monitored with a MouseOx sensor (Starr Life Sciences, Oakmont, PA, USA) beneath the animal's chest. Respiration rate, oxygenation and heart rate varied between 65 to 80

cycles/min, 90% - 100% and 250-320 BMP, respectively, during functional MRI (fMRI) data acquisition.

4. ICA denoising for fMRI data

Independent component analysis (ICA) was applied to decompose the data into 30 components. Components with the following characteristics were identified as noise: 1) signals dominated by a single frequency or by high frequencies above 0.3 Hz; 2) signals with obvious spikes in the time domain; and 3) signals with equal power distribution in the whole frequency range and spatially scattered in the brain. Noise components were regressed out and a bandpass filter (0.01 - 0.25Hz) was applied to the de-noised data before functional connectivity calculation (3).

5. Step-wise regression of CI against "go" and "stop" rsFC

Further step-wise regression analyses indicated that while the "stop" circuit rsFC alone predicted CI, adding the "go" circuit rsFC significantly improved prediction accuracy ($F_{(1,4)}$ change = 11.51, P = 0.027, SI Tables S1 and S2). In contrast, while the "go" circuit alone also significantly predicted CI, adding the "stop" circuit only produced a trend level improvement in prediction ($F_{(1,4)}$ change = 6.08, P = 0.069, SI Tables S3 and S4).

6. Supplementary Figures and Tables

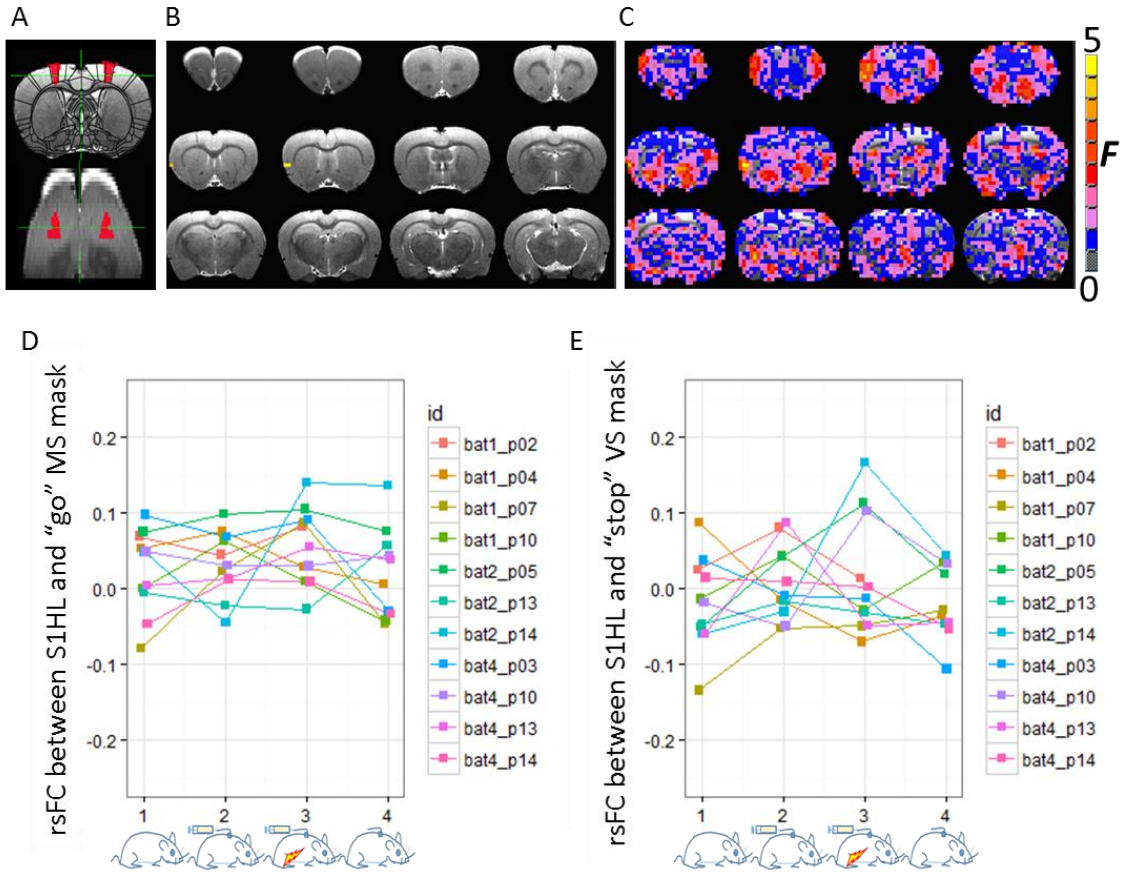

Fig. S1. Control seed analysis. (A) The primary somatosensory cortex hind limb region (S1HL, red color) was chosen as a control seed region whose resting-state functional connectivity (rsFC) was not expected to be impacted by drug as the prelimbic and orbitofrontal cortices. (B) No GROUP-by-SESSION interaction was detected in the S1HL rsFC when controlling for false positive (Note: correction for multiple comparisons requires $p<0.001$ & cluster size >8, herein the cluster of 3 voxels in the figure is considered as false positive). (C) Voxelwise F-stats for the GROUP-by-SESSION interaction without thresholding show negligible effect in most brain regions. (D) Individual rsFC trajectories between S1HL and the "go" medial striatal (MS) mask and (E) between S1HL and the "stop" ventral striatal (VS) mask in the saline group indicate the inter-session stability of the rsFC measure.

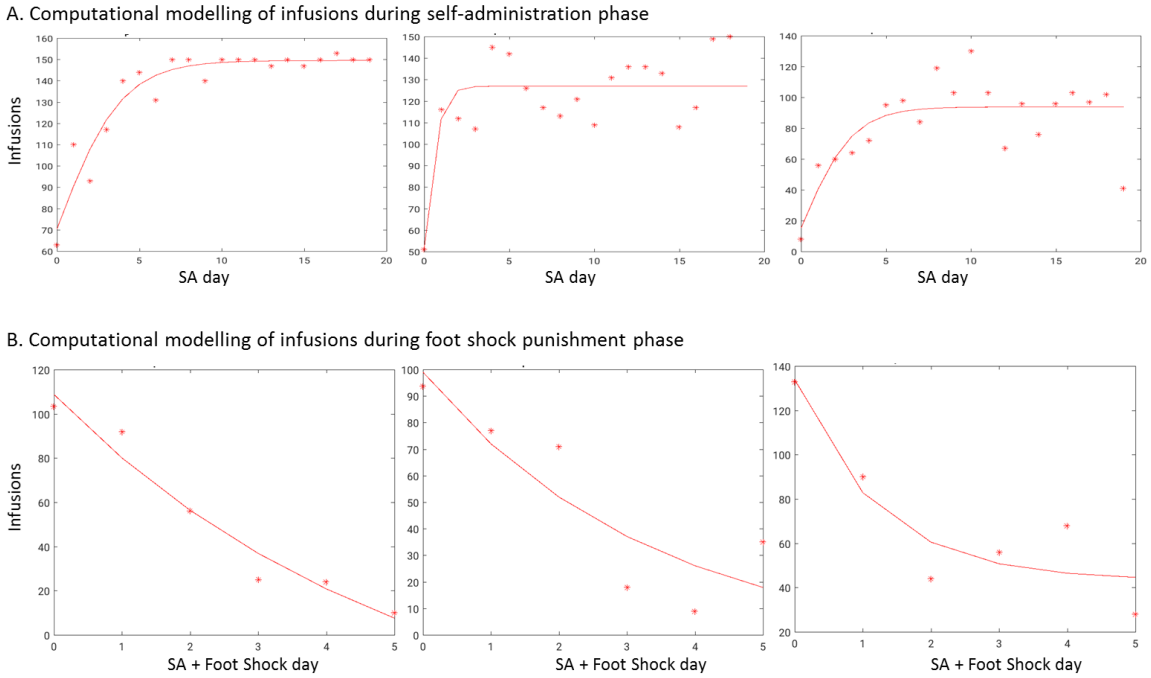

Fig. S2. Examples of computational modelling (solid lines) of drug intake (dots). (A) During the self-administration training phase, some rats showed a small intake variability at plateau (left), but some others showed large day to day variation (middle and right). (B) When foot shock was added to self-administration, some rats showed gradient decrease in drug intake (left) but some others demonstrated large deviations from the decrease trend at the last day (middle and right). Computationally modelling takes all data points into account to estimate an inherent drug taking behavioral pattern.

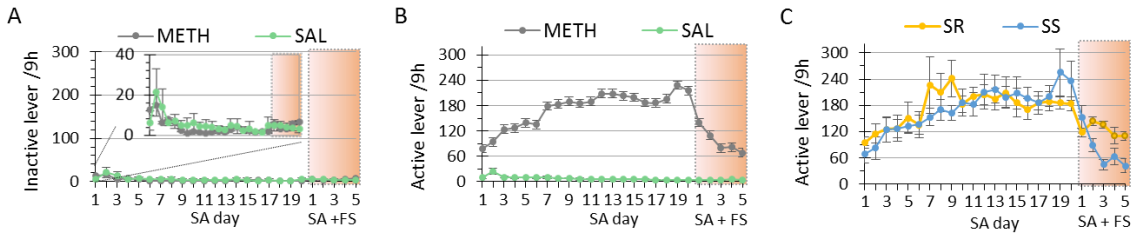

Fig. S3. Lever presses during self-administration (SA) and foot shock (FS) phases. (A) Both methamphetamine (METH) and saline (SAL) rats pressed the inactive lever at a low level. (B) While the SAL group pressed the active and inactive lever similarly, the METH rats escalated the active lever presses during the SA phase and deceased it as a function of foot shock when SA was paired with FS. (C) The shock resistant (SR) and shock sensitive (SS) rats showed similar escalation in active lever presses during SA phase; while both groups reduced lever presses when foot shock was imposed, the SR rats pressed more than did the SS rats.

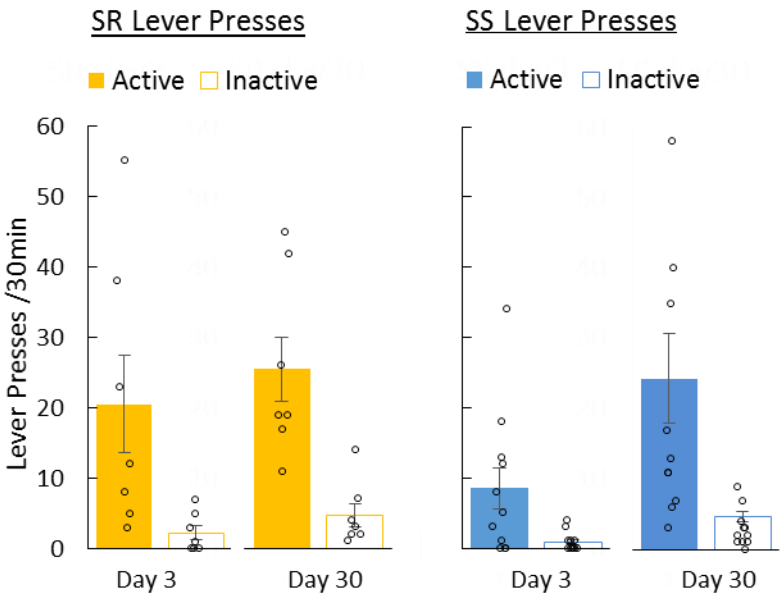

Fig. S4. Lever presses during withdrawal phase. GROUP (SS,SR) x LEVER (Active, Inactive) x Time (Day 3, Day 30) ANOVA analysis indicated that both SS and SR rats pressed significantly more on the active lever (main effect of LEVER, $P < 0.001$); while the rats pressed more at withdrawal Day 30 (main effect of TIME, $P = 0.03$), no significant difference in lever presses change from Day 3 and Day 30 was seen between the two groups (for all GROUP related effects, Ps > 0.27), although the SR rats did press more on the active lever on Day 3 (SR-SS, $T = 1.88$, one tailed $p = 0.04$).

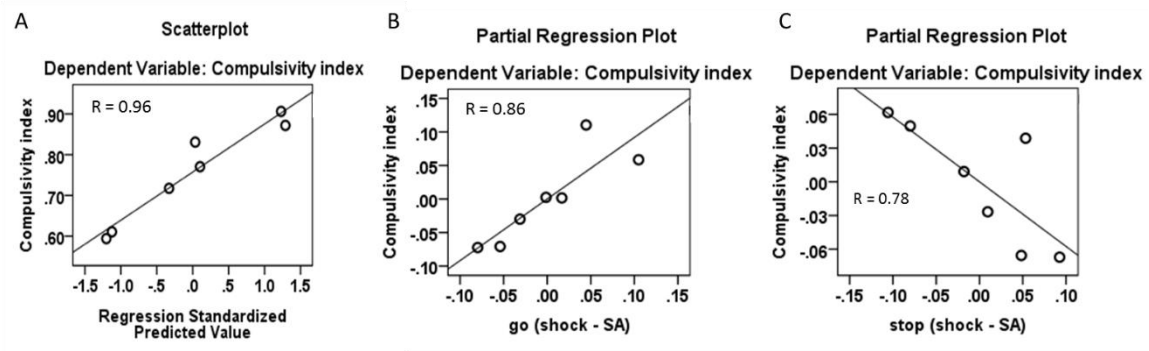

Fig. S5. A multiple regression model predicting compulsive index from OFC ("go") and PrL ("stop") connectivity together. (A) A scatter plot of compulsivity index and predicted values. Partial plots showing that compulsivity index is correlated with connectivity changes from SA to shock in both (B) "go" and (C) "stop" circuits when controlling for each other. Statistics for prediction models are listed in Tables S1-4.

Table S1 the PrL (“stop”) resting-state functional connectivity (rsFC) predicts compulsivity index; adding the OFC (“go”) rsFC significantly improves prediction accuracy

Model	R	R^2	Adj R^2	SE	Change Statistics				
					ΔR^2	ΔF	df1	df2	Sig. F change
1	.839	0.704	0.645	0.073	0.704	11.914	1	5	0.018
2	.961	0.924	0.886	0.041	0.220	11.507	1	4	0.027

Model 1: Predictors: (Constant), change in "stop" rsFC from SA to shock phase
Model 2: Predictors: (Constant), changes in "stop" and "go" rsFC from SA to shock phase
Dependent Variable: Compulsivity Index

Table S2 Coefficients in prediction models 1 and 2 starting with the “stop” resting-state functional connectivity (rsFC)

Model		Unstandardized Coefficients		Standardized Coefficients	t	Sig.	Collinearity Statistics	
		B	Std. Error	(Beta)			Tolerance	VIF
1	(Constant)	.671	.037		18.028	.000		
	“Stop” rsFC(shock-SA)	-1.085	.314	-.839	-3.452	.018	1.000	1.000
2	(Constant)	.781	.039		20.170	.000		
	“Stop” rsFC(shock-SA)	-.575	.233	-.445	-2.466	.069	.585	1.709
	“Go” rsFC(shock-SA)	.918	.271	.612	3.392	.027	.585	1.709

Model 1: Predictors: (Constant), “stop” rsFC(shock-SA)
Model 2: Predictors: (Constant), “stop” rsFC(shock-SA), “go” rsFC(shock-SA)
Dependent Variable: Compulsivity Index

Table S3 the OFC("go") resting-state functional connectivity (rsFC) predicts compulsivity index; adding the PrL ("stop") connectivity has a trend level of significance to improve prediction accuracy

Model	R	R^2	Adj R^2	SE	Change Statistics				
					ΔR^2	ΔF	df1	df2	Sig. F change
1	.899	.808	.769	.059	.808	21.017	1	5	.006
2	.961	.924	.886	.042	.116	6.082	1	4	.069

Model 1: Predictors: (Constant), change in "go" rsFC from SA to shock phase
Model 2: Predictors: (Constant), changes in "go" and "stop" rsFC from SA to shock phase
Dependent Variable: Compulsivity Index

Table S4 Coefficients in prediction models 1 and 2 starting with the "go" resting-state functional connectivity (rsFC)

Model		Unstandardized Coefficients		Standardized Coefficients	t	Sig.	Collinearity Statistics	
		B	Std. Error	(Beta)			Tolerance	VIF
1	(Constant)	.860	.032		27.248	.000		
	"go" rsFC(shock-SA)	1.348	.294	.899	4.584	.006	1.000	1.000
2	(Constant)	.781	.039		20.170	.000		
	"go" rsFC(shock-SA)	.918	.271	.612	3.392	.027	.585	1.709
	"stop" rsFC(shock-SA)	-.575	.233	-.445	-2.466	.069	.585	1.709

Model 1: Predictors: (Constant), "go" rsFC(shock-SA)
Model 2: Predictors: (Constant), "go" rsFC(shock-SA), "stop" rsFC(shock-SA)
Dependent Variable: Compulsivity Index

References

1. Brynildsen JK*, et al.* (2017) Physiological characterization of a robust survival rodent fMRI method. *Magn Reson Imaging* 35:54-60.
2. Cox RW (1996) AFNI: software for analysis and visualization of functional magnetic resonance neuroimages. *Comput Biomed Res* 29(3):162-173.
3. Hsu LM*, et al.* (2016) Constituents and functional implications of the rat default mode network. *Proc Natl Acad Sci U S A* 113(31):E4541-4547.
4. Lu H*, et al.* (2012) Rat brains also have a default mode network. *Proceedings of the National Academy of Sciences of the United States of America* 109(10):3979-3984.